Egyptian Journal of Botany

A Novel *Medicago truncatule* AKT1-null Mutant Impairs Potassium and Sodium Ions Uptake and Affects Root Nodulation

Nahed A.A. Ibrahim[1], Asmaa H. Hassan[2], Omaima A. Sharaf[3], Mohamed E. Saad[2, 4], Shereen F. Elkholy[5, 6], Ghada A. Abu El-Heba[2#]

[1] Department of Microbial Molecular Biology, Agricultural Genetic Engineering Research Institute (AGERI), Agricultural Research Center (ARC), Giza, Egypt; [2]Department of Nucleic Acid and Protein Structure, Agricultural Genetic Engineering Research Institute (AGERI), Agricultural Research Center (ARC), Giza, Egypt; [3]Department of Agricultural Microbiology, National Research Centre, Dokki, Giza, Egypt; [4]Biology Department, Faculty of Science, Taibah University, Almadina Almonawara, Kingdom of Saudi Arabia; (5) Biology Department, College of Science and Humanities, Prince Sattam bin Abdulaziz University, 11942 Alkharj, KSA; [6]Department of Plant Molecular Biology, Agricultural Genetic Engineering Research Institute (AGERI), Agricultural Research Centre (ARC), Giza, Egypt.

REVERSE genetic approach was used to isolate and characterize *Medicago truncatula* containing "knockout" mutations in gene involved in nodulation process and in many other physiological processes. More than 60 *Tnt1*-Flanking sequence tags (FSTs) ranging from ~70bp to ~600bp were isolated, sequenced and submitted to Genebank referring for *akt1* mutant characterization. The proper *Tnt1*-insertion was mapped in chromosome number 8 of *Medicago truncatula* genome. It was precisely identified upstream the base number 141 and downstream of the ATG start codon of *Medicago truncatula* potassium channel *AKT1* gene (MtAKT1). MtAKT1 gene encodes inwardly rectifying potassium channel was isolated, sequenced, and submitted to Genebank with accession number MN649185.1 .*M. truncatula akt1* mutant is achieving higher number of deformed root nodules and shorter root length compared to wild type. *akt1* nodules exhibited reduced size occupied with un-differentiated cells and abnormalities in symbiotic nodule zones. Non-functional nitrogen fixation zone and compacted infection zone were observed as well. AKT1 null mutant exhibits attenuation in its ability to maintain the proper K^+ and Na^+ ions content in *akt1* seedlings which is 2-3 fold less than wild type seedlings,. In contrast, *akt1 seedlings* showed three-fold increase in Ca^{++} ion concentration compared to wild type.

In conclusion *Medicago truncatula* mutant, *akt1* is *Tnt1*-retrotransposon mutant impaired in inwardly rectifying potassium channel AKT1. As the first reported *AKT1* null mutant was isolated from legume plants, this mutant is displaying abnormalities in nitrogen fixation organ and affecting ions uptake.

Keywords: AKT1, FSTs, *Medicago truncatula,* Nodulation process, Potassium channel, Root length.

Introduction

Potassium channels are crucial for different cellular processes in all living organisms. It is essential in plant cell activities, as it is the most dominant solute in the plant cell (Bei & Luan, 1998). Most of the physiological processes, enzymatic activities, guard cell closure, and opening, osmotic regulation are substantially affected by potassium channel (Spalding et al., 1999). Potassium transporter is responsible for regulating its movement across the plasma membrane creating electrical potential variances that can control uptake of other substances (Chrispeels et al., 1999). It is believed that most plants and fungi absorb and accumulate cellular K^+ from the environment via K^+ channels

due to the normally high negative membrane potentials (-120 to -250mV) of the cells (Dennison et al., 2001). Normally, K$^+$ uptake from the soil is going on through two mechanisms, passive and active uptake. Passive uptake is occurring via inward-rectifying channel AKT1 (Sentenac et al., 1992) while active uptake is carried out via KUP/HAK family (Ahn et al., 2004; Qi et al., 2008). *AKT2* (Cao et al., 1995) is a K channel correlated to *AKT1* but is expressed in stems and leaves phloem (Lacombe et al., 2000; Ache et al., 2001; Dreyer et al., 2001). It was found that KAT1, KAT2, AKT1, AKT3/2, and AtKC1 genes encoding inwardly K$^+$ channel subunits mediated stomatal opening and was expressed in guard cells (Szyroki et al., 2001). *Arabidopsis thaliana* channel (KAT1) was first cloned and expressed in *Saccharomyces cerevisiae* and it showed the ability to suppress a K$^+$ transport-impairing phenotype in Saccharomyces mutant cells (Anderson et al., 1992). AKT1 channels are mainly expressed in plant roots (Lagarde et al., 1996) and its activity is efficiently affected by pH and membrane hyperpolarization with a threshold voltage about −120mV. Both AKT1 and KAT1 are plasma membrane proteins sharing homology structure with mammalian K$^+$ channel that belongs to Shaker superfamily. Despite the similarity, both AKT1 and KAT1 are inwardly rectifying voltage-gated K$^+$ channel, while Shaker superfamily channels are outwardly direction (Jan & Jan, 1992).

Insertion mutagenesis is a widely used approach to study functional genomics in model and crop plants (Cowperthwaite et al., 2002; An et al., 2003; Ratet et al., 2006; Mathieu et al., 2009). Mutagenesis can moderate gene expression and generate effectively loss-of-function mutant's lines, and by following the derived phenotypes, gene functions can be explored. *Tnt*1, a Tobacco (*Nicotiana tabacum*) retrotransposon, is an efficient mutagen in *M. truncatula* (El-Sherif et al., 2020), therefore can be utilized in insertion mutagenesis analyses in Medicago plant (D'Erfuth et al., 2003). *Tnt*1 belongs to long terminal repeats (LTR) retrotransposon subclass as it has two direct repeats at both ends. At 5.3kb long and it creates 5bp duplication in the two sides upon the insertion. *Tnt*1 causes stable mutations that successfully can be inherited to the progeny.

AFLP approach was used for mapping the mutation responsible for the derived phenotype of (NF3447 mutant line). The insertion was found inside the AKT1 gene. *akt1* is a *Tnt*1-retrotransposon

mutant harboring nodule architecture abnormality, higher number of root nodules, and shorter root length comparing to wild type. In addition to that, our aim was to isolate and characterize the predicted *Medicago truncatula* potassium channel (MtAKT1) which is the orthologue to *Arabidopsis Thaliana* AKT1 (AtAKT1) and *Oryza sativa* AKT1 (OsAKT1). We used the AFLP-based PCR protocol to screen DNA pools from large numbers of *Tnt*1-mutagenized plants to isolate homozygous "knockout" entities containing a mutation in the gene correlated to the observed phenotype. This kind of reverse genetic approach enables us to isolate significance genes with the unique functions.

Materials and Methods

Plant source

Medicago truncatula mutant NF3447 (Noble Foundation *Tnt*1 mutant collection (Tadege et al., 2008; Sun et al., 2019) was derived from the *Medicago truncatula* R108-1 ecotype. The seeds used for phenotype and genotype experiments were sacrificed and immersed in 10% sodium hypochlorite (Clorox) with vortexing for 5min in 50mL sterile falcon tubes. Sterilized distilled water was used to wash the seeds five times. Seeds were soaked in water with shaking at 50rpm for two days at room temperature. Treated seeds were grown vertically in square plates with nitrate-free BNM medium (Ehrhardt et al., 1992) supplemented by 0.1μM AVG for nodulation test, and the lower part of the plates was enfolded with aluminum foil to reduce roots light exposure. A concentration of 10mM NH$_4$NO$_3$ was added to the BNM media for testing nitrogen tolerance ability in different lines. *sunn* mutant line Tnk100, and R108 wild types were used as positive and negative controls respectively for monitoring hyper nodulation phenotype. *sunn* is an autoregulation of nodulation mutant showing super-nodulation phenotype (Schnabel et al., 2005; Pislariu et al., 2012). Plants were grown in a greenhouse condition at 25°C with 14-hrs./10-hrs. light/dark cycle in 1:1:1 peat moss, perlite, and vermiculite supplemented with NPK fertilizer.

Bacterial strain

Sinorhizobium meliloti strain Sm1021 (Galibert et al., 2001) was grown in tryptone/yeast extract medium at 30°C to an optical density at 600nm and re-suspended in distilled sterilized water to inoculate *Medicago truncatula* plantlets 5 days post-germination. Nodule numbers were scored 15 days post-inoculation. *Escherichia coli* strain

DH5α was used to prepare competent cells used for all DNA transformation protocol and LB medium was used to grow the bacteria with shaking at 37°C/ overnight time.

Nodules examination with light microscopy

Nodules two weeks old were fixed in 100mL solution containing; 50mL ethanol 95%, 10mL formaldehyde, 5mL glacial acetic acid, and 35mL distilled water. Then the fixed nodules were embedded in paraffin wax and the Blocks were divided with the microtome (Euromex USA). Safranin red was used to stain the slides followed by the light green dye. Slides were scanned with the light microscope (Axio vert.A1) according to Zygophyllaceae et al. (2016).

Nitrogenase activity

Root nodules were placed in a sterilized bottle sealed with rubber seal. 10mL of acetylene was injected to replace 10mL of withdrawn air into the same bottle using a plastic syringe. A bottle was incubated for one hour at 30°C. Thereafter liquid chromatography was used for measuring ethylene concentration in a 2mL gas sample (Herbert & Walter, 1972).

Genetic cross

Plants homozygous for the *akt1* allele were back crossed to R108 wild type plants. Entities of the F1 generation were grown and allowed to self-fertilization to produce a population of F2 plants where the mutant alleles were independently segregating. F2 plants were subjected to genomic DNA extraction and PCR amplification to analyze the segregation pattern of *akt1* allele.

Molecular analysis

Tnt1 flanking sequence tags isolation and sequencing

Genomic DNA was isolated from plants according to D'Erfuth et al. (2003). Genomic DNA pool of *akt1* individuals' DNAs was digested with *EcoR*I-*Mfe*I double digestion and *Ase*I-*Nde*I double digestion separately, followed by ligation with ECO and ASE adaptors respectively. AFLP-type PCR was carried out to amplify the *Tnt*1 flanking sequence tags (FSTs). The oligonucleotide primers; LTR3, LTR4, LTR5, and LTR6 for *Tnt*1 borders side while oligonucleotide primers EcoI, EcoII, AseI, and AseII for the adaptor side that were used in the amplification process as well as adaptor sequences was described by Ratet et al. (2006). Thermo scientific fast digest restriction endonucleases

enzymes used in all DNA digestions and TaKaRa T4 DNA ligase is used for ligation reactions. DNA amplifications were done using TaKaRa LA polymerase. *Tnt*1 Flanking Sequence Tags (FSTs) were purified using QIAquick PCR Extraction Kit (Qiagen) and cloned in pGEM-Teasy (Promega) to facilitate fragments sequencing process. FSTs were compared with the sequences of Genebank; http:// blast.ncbi.nlm.nih.gov and Medicago Hapmap; http://www.medicagohapmap.org/home/view Computational Analysis:

The selected protein sequences of AKT1 inwardly rectifying potassium channel were analyzed by using the Basic Local Alignment Search Tool for protein sequences (pBLAST) (Altschul et al., 2005). This tool implements the BLOSUM62 algorithm to compare protein sequences and calculates the statistical significance of matches as means of e-values.

Physiological analysis

K^+, Na^+, and Ca^{++} ions quantification in MtAKT1 null mutant

Five replicas of 15gm dry weight of leaves of both *akt1* mutant and R108 individuals were subjected to K^+, Na^+, and Ca^{++} ion concentration measurements. The measurements were carried out in Regional Center for Food and Feed, ARC, Giza, Egypt.

K^+ depletion assay

Seven days old seedling grown in MS media were exposed to medium containing 0μM, 100μM, 1000μM K^+ with and without the addition of 2 mM NH_3. The weight of five replicas for each concentration was recorded regularly to correlate the change of *akt1* mutant growth rate by using different low concentration K^+ containing media comparing to R108. The different K^+ and NH_3 concentrations were added to MS-free K^+ media.

Statistical analysis

The mean values of 10 replicas were calculated for each treatment and used in data analysis by Graphpad prism7. Data for each treatment was analyzed by the TWO-WAY ANOVA (P≤ 0.05) method.

Results

akt1 Phenotype

Evaluation of the phenotype of a gene null mutant is a powerful approach for studying gene

function. An *akt1* mutant was tested against the super-nodulating mutant *sunn* and R108 wild type as two controls for phenotype reporting. Root length variation was observed in one-week-old seedlings in the three lines. *sunn* exhibited the shortest root length followed by *akt1* then R108. The root length mean values for 12 days old seedling were 1.5cm, 3cm, and 5.6cm for *sunn, akt1,* and R108 respectively (Fig. 1). For testing *akt1* Nodule Phenotype, seven-days-old Medicago seedlings were inoculated with nitrogen fixing bacteria (*Sinorhizobium meliloti).* Nodule phenotype was detected one month-post inoculation and nodules number was counted. *akt1* nodule was showing abnormalities comparable to the wild type R108 as non-fixing phenotype and nodule numbers count was 25±5, 15±5, and 10±5 for *sunn*, *akt1,* and R108, respectively. *akt1* mutant did reveal nitrogen-tolerant symbiosis phenotype as that displayed by *sunn* mutant on 5mM NH_4NO_3 supplemented-MS medium. *akt1* nodule exhibited reducing size occupied with un-differentiated cells and abnormalities in symbiotic nodule zones. The infection zone appeared as a compacted and un differentiated non-functional nitrogen fixation zone (Fig. 2).

Mutant isolation and identification

Two nested PCR reactions were carried using DNA pool of *akt1* ligated to the proper adaptors (Ratet et al., 2006) and the products were separated on a 1.5% agarose Tris-acetate EDTA gel running at 80 V. (Fig. 3). More than seventy fragment sequence tags FSTs were cloned in pGEM T-easy vector, sequenced, and analyzed for homologs similarity. 28% of the cloned fragments exhibited very

high similarity with coding regions of *Medicago truncatula*, *Cicer arietinum,* or *Trifolium pratense* genome, while 21% are repeated sequences and 2.5% with no matching. FSTs are shown in Suppl. Table. FSTs corresponding to *akt1* were submitted to Genbank http://www.ncbi.nlm.nih. gov/. **Genbank accession numbers; KT001939, KT001939, KT001940 KT001941, KT001942, KT001943, KT001943, KT001943, KT001944, KT001945, KT001946, KT001947, KT001948, KT001949, KT001950, KT001951, KT001952, KT001953, KT001954, KT001955,** the E-value and the matching reference genes are shown in (Table 1). Short tagged sequences without accession numbers are shown in Table 2. Following data analysis, eight *Medicago truncatula Tnt1* insertion sites were subjected to further investigation; For HYPN_1 insertion, for HYPN_52 insertion, for HYPN_2 insertion, for HYPN_9 insertion, for HYPN_7, for HYPN_57, for HYPN_15, for HYPN_512: H22. These designed oligonucleotide primers were used to investigate *Tnt*1 insertion pattern in terpene synthase (TPS5), phosphoribosyl transferase-like protein, EF hand family protein, (9E) locus, Polygalacturonase-1 non-catalytic, Malonyl-CoA isoflavone 7-O-glucoside-6'-O-malonyl transferase, (G18) locus, and Dopamine beta-monooxygenase respectively as shown in Table 3. Genomic DNAs were extracted from F2 population entities resulting from *akt*1 mutant & R108 back crossed, and only entities showing the described mutant phenotype were tested (about 1/4 population of the F2 progeny). PCR results indicated that insertion on those loci was not charged for the mutation phenotype. Results are shown in Suppl. Figs. 1-8.
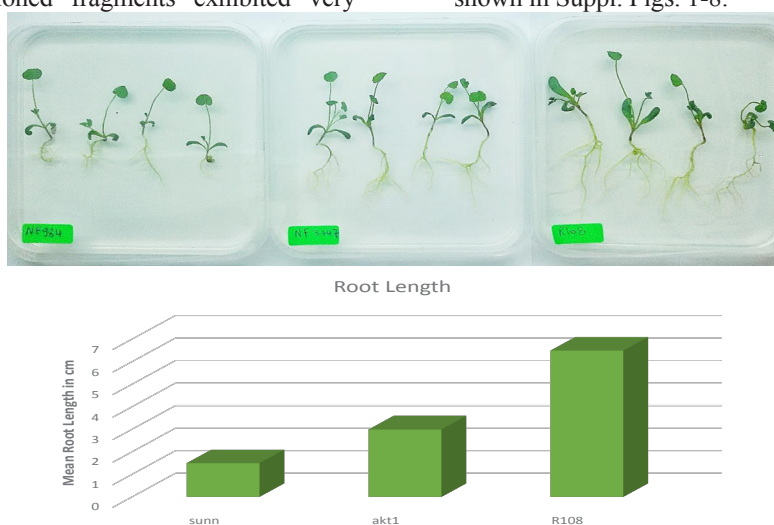

Fig. 1. Root Length in one-week old Medicago seedling of NF984 (*sunn* mutant), NF3447 (*akt1* mutant) and R108
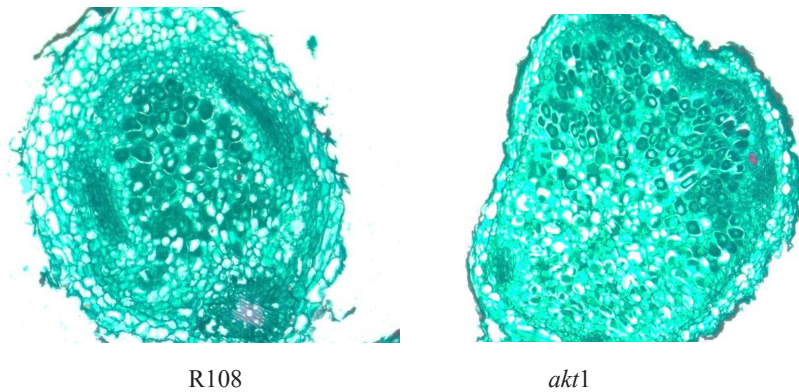
Fig. 2. One-month old nodules longitudinal sections of *akt1* mutant displayed reduced size nodule with decreased number of nodule's cells and clear aging symptoms [Cells exhibited clear un-differentiation and compacting in both infection and nitrogen fixation zones compared to R108 wild type]
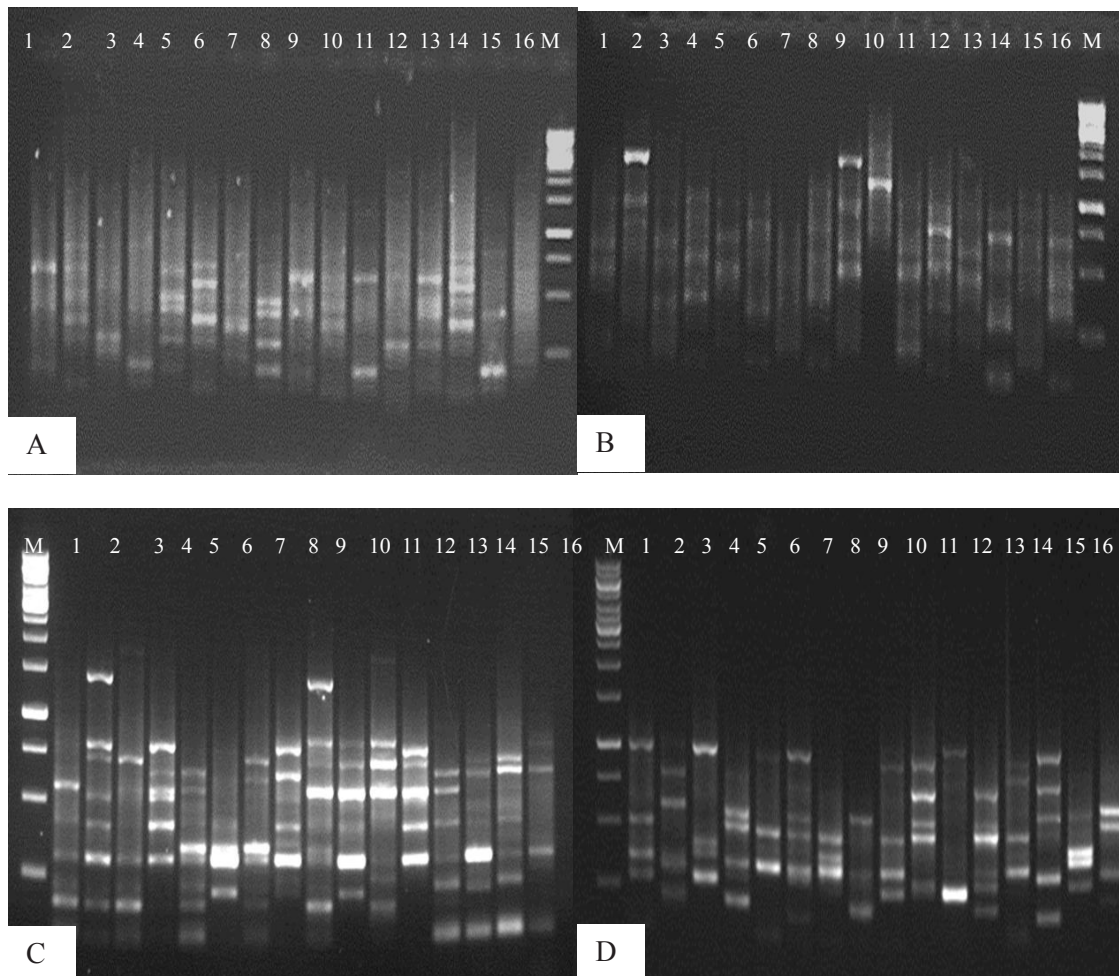

Fig. 3. A) *EcoRI&MfeI* **PCRII products using EcoR2 and LTR4 oligonucleotide primers, (B)** *EcoRI&MfeI* **PCRII products using EcoR2 and LTR6 oligonucleotide primers, (C)** *AseI&NdeI* **PCRII products using Ase2 and LTR4 oligonucleotide primers, (D)** *AseI&NdeI* **PCRII products using Ase2 and LTR6 oligonucleotide [Lane from 1-16 are AA, AC, AG,AT,CA,CC,CG,CT,GA,GC,GG,GT,TA,TC,TG,TT, respectively at the end of Eco2 and Ase2 oligonucleotide primers]**

TABLE 1. *akt1* corresponding FSTs accession numbers

Sequence name	Length	Accession number	Organism	Reference	E-value
HYPN_1	200	KT001939	Medicago truncatula (MTR_064s0024) (+)-delta-cadinene synthase isozyme A	gb|DQ188184.1	9e-32
HYPN_2	226	KT001940	Medicago truncatula EF hand family protein (MTR_3g101600) mRNA	ref|XM_003602984.1	2e-113
HYPN_3	511	KT001941	Medicago truncatula adenosylhomocysteinase (AHC2) gene	gb|AY224189.1	0.0
HYPN_4	265	KT001942	Trifolium pratense genome assembly redclover, chromosome	emb|LN846349.1	4e-12
HYPN_5	292	KT001943	Cicer arietinum uncharacterized LOC101501738 (LOC101501738), mRNA	ref|XM_004488278.1	1e-82
HYPN_6	234	KT001944	Medicago truncatula Anthranilate phosphoribosyltransferase-like protein (MTR_4g071870) mRNA	ref|XM_003607018.1	5e-104
HYPN_7	652	KT001945	Medicago truncatula Polygalacturonase-1 non-catalytic subunit beta (MTR_5g034320) mRNA	ref|XM_003613186.1	0.0
HYPN_8	208	KT001946	No matching	-	-
HYPN_9	312	KT001947	No matching	-	-
HYPN_10	578	KT001948	Medicago truncatula clone mth2-133k2	gb|AC147537.39	5e-134
HYPN_11	219	KT001949	Medicago truncatula UDP-glucuronosyltransferase 1-6 (MTR_7g102550)	XM_003625674.1	1e-108
HYPN_12	500	KT001950	No matching	-	-
HYPN_13	334	KT001951	No matching	-	-
HYPN_14	450	KT001952	Medicago truncatula clone mth2-151m16	gb|AC147002.20	9e-51
HYPN_15	200	KT001953	Medicago truncatula clone mth2-27d4	gb|AC144656.12	8e-88
HYPN_16	450	KT001954	Medicago truncatula clone mth2-8o7	gb|AC145331.19	0.0
HYPN_17	252	KT001955	M.truncatula DNA sequence from clone MTH2-173L20 on chromosome 3	emb|CU062422.10	4e-87

Medicago truncatula AKT1 encodes inwardly rectifying potassium channel is interrupted by Tnt1-insertion

*AKT*1 specific oligonucleotide primer for H24R: 5'-CCAATGACTATGTGTGGCCAA-GA-3' was designed and used against LTR4 oligonucleotide for *Tnt*1 border to investigate the *Tnt*1 incidence in the predicted mutated locus, AKT1 potassium channel. PCR result detected the *Tnt*1 insertion in the proper locus for all F2 entities showing the mutation phenotype while it appears in 2/3 of the entities showing wild type phenotype (examples are shown in Suppl. Fig. 9). *Medicago truncatula* potassium channel *AKT1* gene (MtAKT1) is 7286bp and it encodes inwardly rectifying potassium channel with a length of 888 amino acids (**accession number MN649185.1).**

The insertion was detected on chromosome eight of Medicago genome just upstraem the base number 141 and downstream of the ATG start codon of *AKT1* gene. MtAKT1 3D structure modelling based on Swiss Model https://swissmodel.expasy.org/interactive is shown in (Fig. 4). AKT1-N-terminal contains partially homologous and structurally analogous sequences to Shaker superfamily transmembrane domain of voltage-gated channels (Fig. 5). This channel response to changes in cell membrane voltage by allowing ion conduction to their C-terminal ends. The other domains are the putative cyclic nucleotide-binding domain, ankyrin-repeat domains (Fig. 6) homologous to human erythrocyte ankyrin. The last domain is a conserved C-terminal KHA domain that is unique to plant K+ channels. The KHA domain encloses

two high-homology blocks enriched for hydrophobic and acidic residues, respectively. The KHA domain is essential for interaction of plant K (+) in channels. The KHA domain mediates tetramerization and/or stabilization of the heteromers. A phylogenetic tree was assembled using ClustalW2_phylogeny EMBL-EBI MtAKT1. *Medicago truncatula* inwardly rectifying potassium channel is an ancestry related to *Cicer arietinum* potassium channel AKT1, *Lupinus angustifolius* potassium channel AkT1-like and *Vigna radiate* potassium channel AKT1 (Fig. 7). Oligonucleotides primers used for AKT1 sequencing are; POT1-F: 5'-CGCGGATCCCATAAAAATGGT-GCTTCC-3', POT1R:5'CCGGAATTCCACATT ATGAATTGACACC-3', POT2-F: 5'-CGGCTT-GAGAAGGACAGAAACTATAA-3', POT2-R: 5' CTTGATGCAGCTTGTATGGTATCCC-3', POT3-F: 5'-GTCAAATTCCTATTAGAACATG-GT-3', POT8F: 5'-CCAAGTCATATTTTGTA-AGTC-3', POT5R: 5'-CATTGGTACTAAAT-GCAATC-3' POT9F 5'-CAAATTGGGGAT-GTTGGTCA -3', POT6R: 5'-TCGCTTTG-TATTTATGTAAAT-3' POT10F:5'- GGATTCT-CAACTGAAATTCCT-3', POT11F: 5'-GTT-GTACAAAATGGTTGTAC-3'POT12F:5':- G

ATTCTTTGCTATAGATATAGT-3', POT7R: 5'-AGCATCCAGCACAGTGCACAGC-3'

Medicago truncatula akt1 is impairingin K⁺, and Na⁺ ions uptake while Ca⁺⁺ ion permeability is increased

AKT1 null mutant exhibited attenuation in its ability to maintain the proper K^+ and Na^+ ion content. R108 seedlings showed almost two to three fold folds increase in K^+ and Na^+ respectively compared to *akt1* seedlings as shown in (Fig. 8). *akt1* showed a three-fold increase in Ca^{++} ions concentration compared to R108 wild type seedlings (Fig. 9). This elevation could be a substitution response due to the dramatic reduction of potassium and sodium ions level.

K⁺ affects akt1 leave dry weight

One of the most important characteristics of *akt1* mutant is a 40% reduction in dry weight compared to R108 wild type at the same age and under the same growing conditions. This significant reduction is in consensus with our findings in the decrease of K^+ uptake due to potassium channel mutation.

TABLE 2. *akt1* corresponding short FSTs

Sequence name	Length	Accession number	Organism	Reference	E-value
HYPN_52	100	-	Medicago truncatula Anthranilate phosphoribosyltransferase-like protein (MTR_4g071870) mRNA	ref|XM_003607018.1	1e-37
HYPN_53	86	-	Medicago truncatula UDP-glucuronosyltransferase (MTR_6g014190)mRNA,	gb|AC135100.12	3e-34
HYPN_54	196	-	Medicago truncatula clone mth2-70l3	gb|AC166898.17	4e-92
HYPN_55	158	-	Medicago truncatula chromosome 5 clone mth2-179e23	emb|CU326389.1	4e-65
HYPN_56	155	-	Medicago truncatula UDP-glucuronosyltransferase (MTR_6g014190) mRNA	ref|XM_003618608.1	7e-68
HYPN_57	74	-	Medicago truncatula Malonyl-CoA isoflavone 7-O-glucoside-6'-O-malonyltransferase (MTR_7g014360) mRNA	ref|XM_003621428.1	-3e-23
HYPN_58	29	-	Medicago truncatula chromosome 7 clone mth2-81g19)	gb|AC153128.1|	0.075
HYPN_59	104	-	Medicago truncatula chromosome 2 BAC clone mth2-18p14	gb|AC198006.2	5e-35
HYPN_510	134	-	-	-	-
HYPN_511	150	-	Medicago truncatula clone mth2-22g6	gb|AC141108.3	2e-33
HYPN_512	107	-	Medicago truncatula Dopamine beta-monooxygenase (MTR_5g093520)	ref|XM_003617565.1	1e-41

TABLE 3. *Medicago truncatula Tnt1* insertion sites and their specific oligonucleotides

| Tnt1 insertion sites	Oligonucleotides sequences	Source
HYPN_1	3AF: 5'-GATCTTCAATTGGGTATCAAATGA-3'3AR: 5'-AGGCATCGGAACTTCGGTTGGCCT-3'	terpene synthase (TPS5)
HYPN_52	16AF: 5-ATGTTTCAGATCGACAGTCTGCGA-3' 16AR: 5'-TAGCGGCAAAATAGCTCCCGGCTT-3'	phosphoribosyl transferase-like protein
HYPN_2	35BF: 5'-ATGCCGTTCATGGATCACAAAGGG-3' 35BR: 5'-CGTTATGATTGGTGTCTGCAGCGT-3'	EF hand family protein
HYPN_9	9EF: 5'-TCACGGCGAGGATCTTTACTTCCT-3' 9ER: 5'-TTGACTTCCACGTGTCAGTCACTG 3'	(9E) locus
HYPN_7	5CF: 5'-AGAGATAAATTACCTAAAAGGTCG-3'5CR: 5'-GAACCACCACATTTCGACCCAAAA-3'	Polygalacturonase-1 non-catalytic
HYPN_57	25CF: 5-TGTCGGACTCGTTTAGATCAGCCA-3' 25CR: 5'-AATGAAGACCAATTTTCAGCTCCA-3'	Malonyl-CoA isoflavone7-O-glucoside-6'-O-malonyl transferase
HYPN_15	G18F: 5'-CAGGATCAACATACATGTGCTTTG-3' G18R: 5'-CTCATCTTCAAACTTCTTCTTCCA-3'	(G18) locus
HYPN_512	H22F: 5'-CGCAGCCGGGGACAGAAGCTGAGT-3'H22R: 5'-TCCGGTAATCATCTGTCGACTTGG-3'	Dopamine beta-monooxygenase respectively
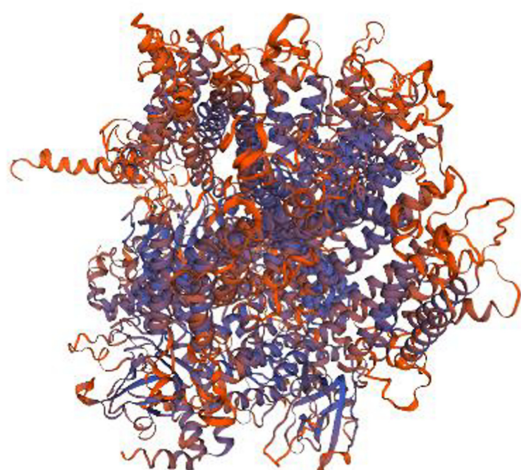
Fig. 4. 3D structure modelling AKT1 protein based on Swiss Model
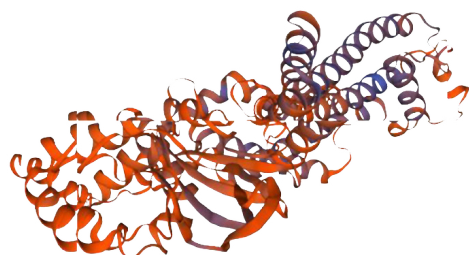

Fig. 5. 3D structure modelling of transmembrane domain of voltage gated channel based on Swiss Model
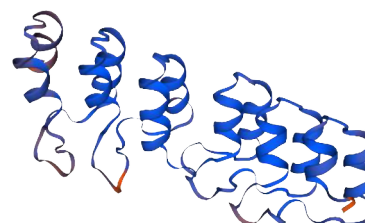

Fig. 6. 3D structure modelling of ankryin-repeat domain based on Swiss Model

K⁺ affects akt1 mutant growth and survivability

AKT1 null mutant growth rate was measured against wild type using 0μM, 100μM, 1000μM K⁺-containing media. This experiment was duplicated with the addition of 2mM NH_3 in addition to the different K⁺ concentrations. NH_3 acts as non-AKT potassium uptake pathway inhibitor by competing for K⁺ binding sites (Spalding et al., 1999). Figure 10 showed that in the absence of NH_3, the growth rate of wild-type seedlings increase with increasing K⁺ concentration in growth media, thus in normal condition the growth rate increase by increasing potassium availability. *akt1* showed an obvious slower growth rate at 100μM, 1000μM K⁺ than wild type, while *akt1* was recording higher values of fresh weight than the wild type on 0μM K⁺ at first, second and third week. On the other hand, R108

was recording higher values than *akt1* at 100μM K$^+$, 1000μM K$^+$ at first, second and third week as well. This data was in agreement with our observation of *akt1* behavior on 0μM K$^+$ containing medium as the root on harsh K$^+$ depletion condition become more condensed and dispersed on the growth media. One-month wild type seedlings grown on 0μM K$^+$ with and without 2mM NH$_3$ exhibited chlorosis and declining symptoms prior to death compared to *akt1* which showed more tolerance and survived on K-neutral conditions (Fig. 11, Suppl. Fig. 10).

Effect of 1-aminocyclopropane-1-carbxylic acid (ACC), 1-Naphthaleneacetic acid (NAA) exogenous addition on akt1 root growth

Phytohormones have a fundamental role in plants growth, development, rooting initiation and lateral root development. Previous data proposed that auxin and ethylene are the major regulators of root phenotype (Cherel et al., 2014). The ability of ACC and NPA in affecting *akt1* root growth in a manner that is likely to occur in *sunn* was tested. Medicago wild type and *sunn* mutant was used as negative and positive controls, respectively. 0.1μM. 1μM, 10μM ACC and 0.1**μM**. 1**μM**, 10**μM** NAA exogenous additions were applied separately to MS growth media. Root lengths of five seedlings for

each line were recorded every 3 days' time intervals. The *akt1* plants has the highest root length on 10μM ACC-containing media recording 10cm opposed to 7.8cm and 5cm for R108 and *sunn* respectively, indicating that ethylene did not influence *akt1*. *sunn* plants were unaffected by ACC addition as it kept the shortest root phenotype which is the one of the common characteristics of this mutant while wild type root growth was inhibited by the addition of 10μM than 0.1μM and 1μM of ACC. The relative inhibitory effect was detected by applying an elevated NAA concentration in *akt1*, *sunn*, and wild type as well (Figs. 12, 13). The assessment of exogenous plant hormone confirms that *akt1* was responding in a manner different from *sunn* with ACC treatment, while it showed somehow similar effect with NAA treatment. Decreased nodule numbers were also observed on *N*-(1-naphthyl) phthalamic acid (NPA)-treated *akt1*, *sunn*, and wild type on one-month post Rhizobia infection. This inhibition in nodule formation was the highest in *sunn*, followed by *akt1* and the lowest in wild type (Fig. 14). That means the potassium uptake deficiency can disturb root growth and nodulation initiation process like *sunn* which has shoot LRR-RLK-signal perception defect but in a different way.
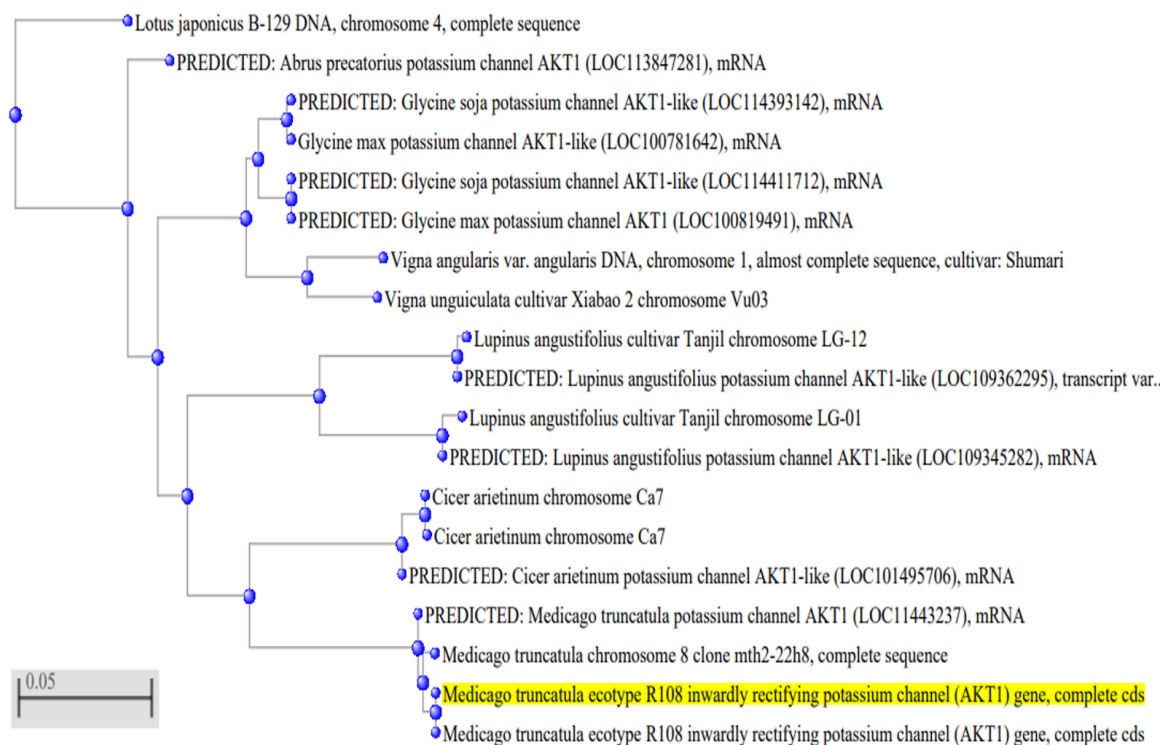

Fig. 7. Neighbor-joining method Phylogenetic tree for *Medicago truncatula* MtAKT1 Inwardly rectifying potassium channel using ClustalW2_phylogeny EMBL-EBI
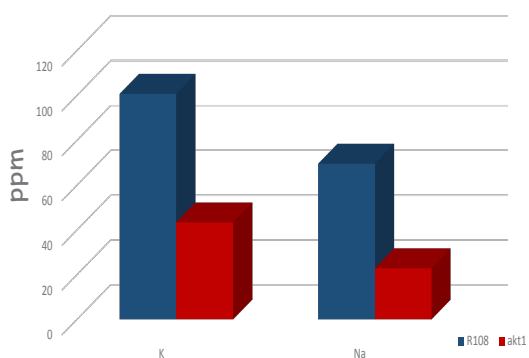
Fig. 8. K$^+$ and Na$^+$ ions contents measurement in *akt1* and R108 [K$^+$ and Na$^+$ ions contents in R108 is triple and double folds contents, respectively compared to *akt1* seedlings]
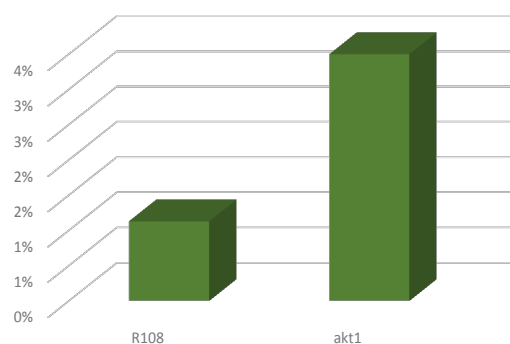

Fig. 9. Ca^{++} content measurement in *akt1* and R108 [*akt1* showed increase in Ca^{++} ions concentration three times more than R108 wild type seedlings]
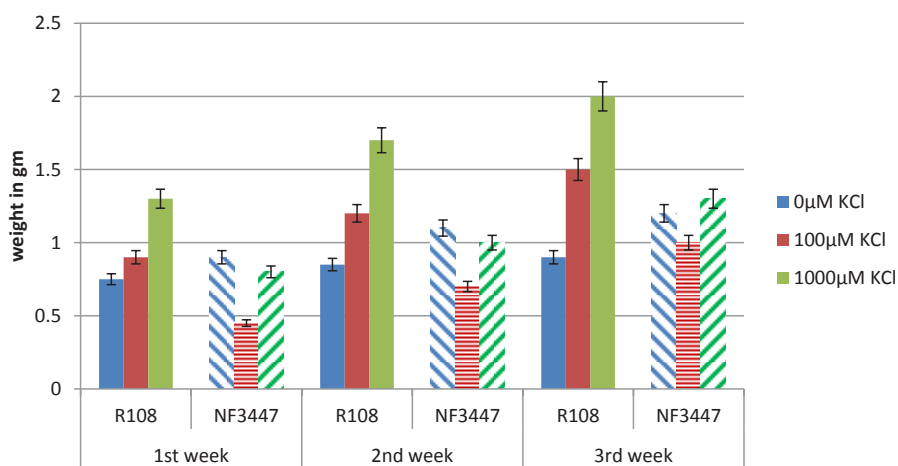

Fig. 10. Effect of Low K$^+$ cotaining Media on *akt1* and R108 seedlings growth [Growth rate of R108 wild-type seedlings increase with increasing K$^+$ concentration in the growth media. *akt1* showed slower growth rate at 100μM K$^+$, 1000μM K$^+$ than wild type. At 0μM K$^+$ *akt1* was recording the highest values of fresh weight compared to wild type at the first, second and third week]
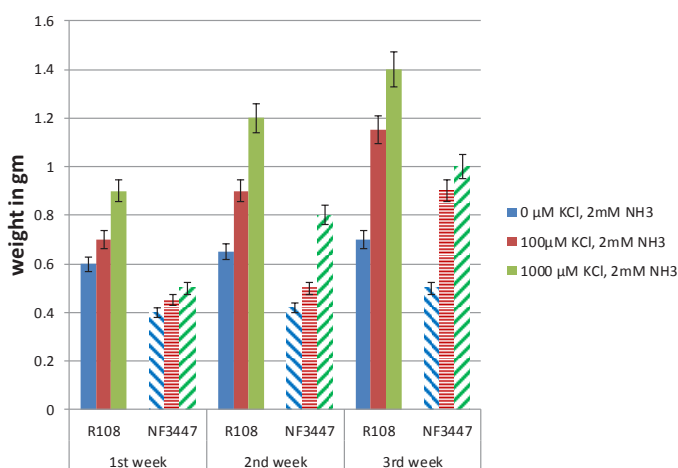

Fig. 11. Effect of Low K with NH$_3$ cotaining Media on *akt1* and R108 plants growth [2mM NH$_3$ containing media was used to block the non-AKT potassium uptake pathway. *akt1* showed a lower growth rate than R108 wild type on 0μK$^+$, 100μM K$^+$, 1000μM K$^+$]

Fig. 12. Effect of ACC exogenous addition in *akt1* mutant root growth using concentrations of (A) 0.1µM, (B) 1µM, (C) 10µM [Each point represent the mean value of 5 plants' lengths. R108 wild type and *sunn* mutant were used as negative and positive controls, respectively]
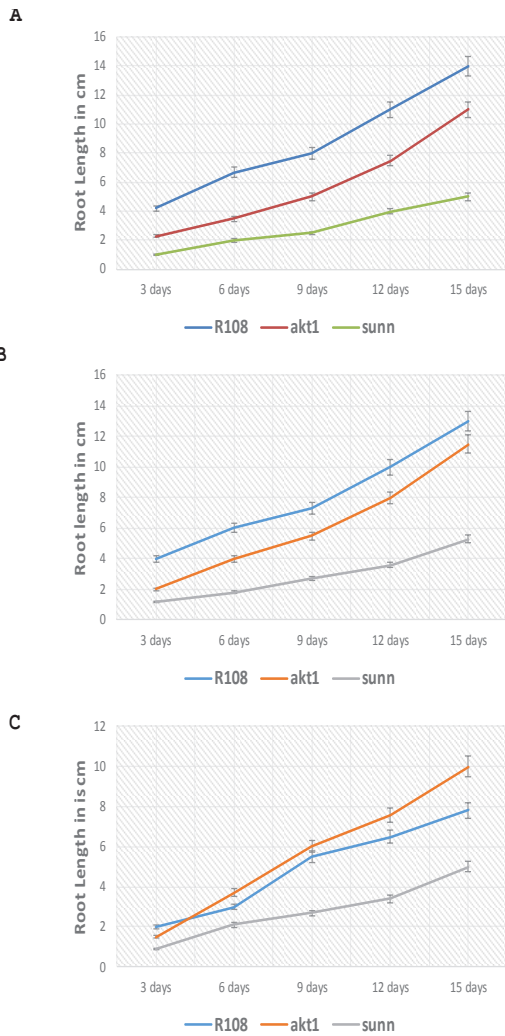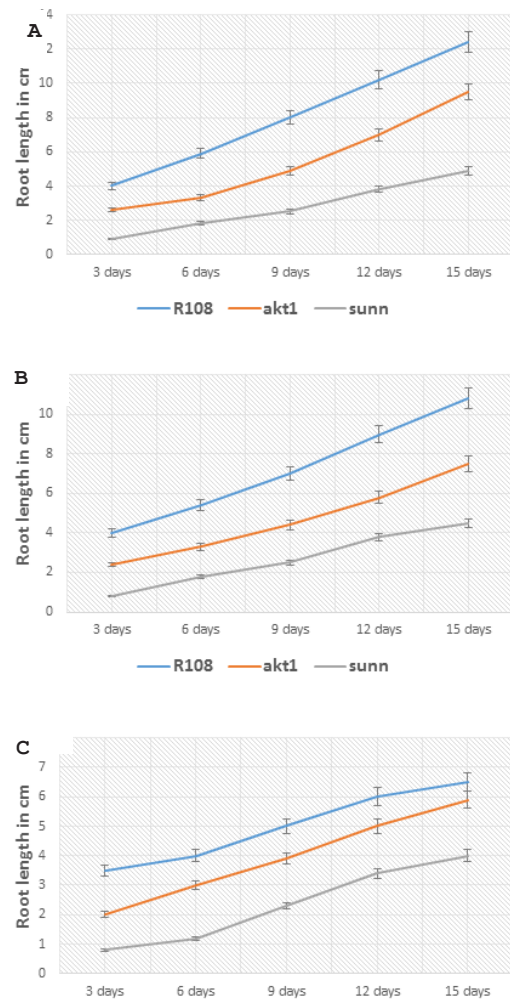
Fig. 13. Effect of NAA exogenous addition in *akt1* mutant root growth using concentrations of (A) 0.1µM, (B) 1µM, (C) 10µM [Each point represent the mean value of 5 plants' lengths. R108 wild type and sunn mutant were used as negative and positive controls, respectively]
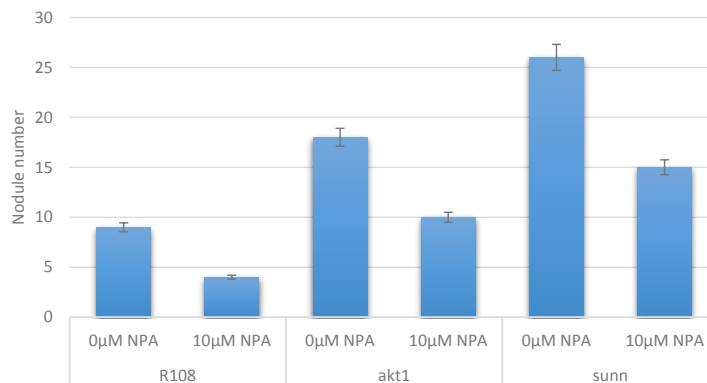

Fig. 14. Effect of 10µM NPA exogenous addition in nodule number [Nodule formation inhibition was observed on N-(1-naphthyl) phthalamic acid (NPA)-supplemented media in *sunn*, followed by *akt1* then the R108 wild type]

Discussion

Potassium is a crucial nutrient for plants growth, metabolism, development, and yield (Clarkson & Hanson, 1980; Cao et al., 2007; Marschner & Marschner, 2011; Loutfy et al., 2019). Due to the extended duration of crops in cultivated land and due to low and unstable concentration of potassium ion in soil (Schroeder et al., 1994), a shortage in potassium content might be experienced (Pettigrew, 2008; Jin, 2012). K^+ deficiency can lead to a dramatic reduction in crop production and a decrease in quality. Compensation by potassium fertilizers is an economic and environmental burden. Understanding the molecular aspects of potassium uptake and interplay between potassium and other phytohormones signals is of great value. Studying *Medicago truncatula* impaired in K^+ uptake can elucidate the physiological mechanism of potassium deficiency tolerance and the subsequent potassium deficiency phenotype. Our data reveals that *Medicago truncatul akt1* mutant is displaying fix- nodule with increasing nodule numbers, shorter root length, and a decrease in dry weight compared to wild type plants. This novel mutant doesn't fall into the group of previously described *sunn*, autoregulation of nodulation (AON) mutant or ethylene-insensitive superernodulating mutant, *sickle* (*skl*) (Prayitno *et al*., 2006). The first concern in AKT1 mutant (*akt1*) characterization was determination of root K^+ contents under normal growth condition with the availability of enough nutrients. Results indicated that K^+ and Na^+ were significantly reduced in *akt*1 mutant compared to wild type, in contrary to Ca^{++} which was significantly increased in *akt1* compared to the wild type. Our results indicated that AKT1 not only mediates K^+ uptake but Na^+ uptake as well.

We hypothesize that AKT1 channel is involved in potassium and sodium ions uptake. Calcium ion level may be elevated as a substitution response due to the dramatic reduction of potassium and sodium levels. When growing in soil replete with the proper nutrient contents, *akt1* is clearly displaying short root and low growth rate phenotype compared to wild type. In order to observe *akt*1 response growing on low K-containing media, *akt1* and wild type were exposed to low concentration of K-supplemented media starting from zero potassium concentration. Despite the higher fresh weight values recorded by *akt1* than the wild type at 0µM K^+, *akt1*

seedlings were growing significantly slower than wild type on 100µM K^+, 1000µM K^+. This data is similar to Hirsch et al. (1998). He proofed that the root growth rate of *akt1-1 Arabidopsis* mutant is strongly reduced compared to wild type in low limiting potassium containing media. While both *akt1* and wild type exhibited root growth inhibitory effect with the addition of NH_3, the non-AKT1 blocker, this inhibitory effect is eliminated with an increasing K^+ level in the growing media. Our findings are opposite to that of rice, where the NH_3 addition didn't show growth inhibitory effect on rice *akt1* KO mutant (Ahmed et al., 2016). While our findings agree with Arabidopsis *akt1-1* which is lacking the activity of inward-rectifying K^+ channel and exhibited a significantly K^+ permeability reduction through the plasma membrane, and slowly growing than wild type on K^+-limiting media (Dennison et al., 2001).

Root architecture moderates to grow towards K^+ rich zones, this fact can explain the expansive growth rate of Medicago *akt1* seedling on 0µM K^+ concentration without NH_3-addition than wild type. This higher growth rate is due to root extension, condensation and dispersion on the growth media in a trial to survive and find potassium in the surrounding. In our case wild type growth almost stop and this response is what commonly occurs during potassium deficiency (Hodge 2004; Gruber et al., 2013; Cherel et al., 2014). Generally, different plant genotypes display different responses in primary and lateral root growth under condition of low potassium (Kellermeier et al., 2013). Xu (2006) showed a similar result with Arabidopsis *akt1* mutant in which primary root continues to grow, while root growing is halted in wild type at K deficiency condition.

Phytohormones; auxin, cytokinin, ethylene, and jasmonic acid are involved in plant's response to nutrients insufficiency (Armengaud et al., 2004; Wang & Wu 2013; Bensmihen, 2015). Auxin and ethylene are major regulators of root phenotype (Cherel et al., 2014). Ethylene or the ethylene precursor is acting as a stimulator for auxin biosynthesis and regulating its transportation mechanism by transactivating the activity of most components involving in auxin transport (Stepanova et al., 2005; Ru' zickaet et al., 2007). ACC exogenous addition inhibited wild type root growth and the inhibitory effect is directly proportionate to increasing ACC concentration in

the growth media, while it failed to show strong inhibitory effect with *akt1* and *sunn*. In consensus with ethylene production increase and its related genes are trans-activated during K⁺ deficiency (Shin and Schachtman 2004), *akt1* is thought to have excessive amount of ethylene to a limit that the exogenous addition couldn't show more inhibition effect than which already in existence. Whereas *akt1* showed a little inhibitory effect than wild type while *sunn* showed the least inhibition influence. Surprisingly, NAA exogenous addition inhibited *akt1* root growth in a manner similar to wild type. NAA inhibitory effect increased by increasing the hormone concentration for the *akt1* and wild type. The least inhibitory effect was displayed by *sunn* as it maintained its short root phenotype and appeared with its normal averages of root lengths for this stage of seedling life. This research can contribute in finding out new strategies to decrease the use of K⁺ fertilizers and improve plant's nutrition uptake aiming to improve field production quality.

Conclusion

Medicago truncatula AKT1 inwardly rectifying potassium channel is involved specifically in potassium and sodium ions uptake. AKT1 activity is influencing other regulator like auxin and ethylene. AKT1 is involved in root growth determination and nodulation process. *Medicago akt1* exhibited short root phenotype and increasing nodule number than the wildtype R108 on growth media or in soil, contrary to Arabidopsis *akt1* which displayed the shorter root phenotype when grown on K-limiting media only (Wang et al., 2016). *akt1* showed more tolerance and survived K- deficiency than wild type, similar to *Arabidopsis akt1*. *akt1* nodule is fix- with undifferentiated cells and abnormal compacted infection and nitrogen fixation zones showing early aging symptoms. *Medicago akt1* respond differently than *sunn* in K-ambient condition and with different exogenous hormone treatments as well.

List of abbreviations: MtAKT1*: Medicago truncatula* potassium channel *AKT1* gene, PCR: Polymerase chain reaction, RT-PCR: Reverse transcription-polymerase chain reaction, K⁺: Potassium ion, Na⁺: Sodium ion Ca⁺⁺: Calcium.

Conflict of interests: The authors declare no conflict of interest.

Authors contributions: NI performed work related to AFLP, AH performed physiological experiments, SE performed the computational analysis and revised the manuscript , OS was responsible for analyzing the data, MS performed AKT1 gene sequencing and assembly, revised the manuscript, and GA supervised the research and performing bioinformatics analysis. All authors read and approved the final manuscript.

Ethical approval: Not applicable.

References

Ache, P., Becker, D., Deeken, R., Dreyer, I., Weber, H., Fromm, J., Hedrich, R. (2001) VFK1, a *Vicia faba* K+ channel involved in phloem unloading. *Plant Journal*, **27**, 571–580.

Ahmad, I., Mian, A., Maathuis, F.J. (2016) Overexpression of the rice AKT1 potassium channel affects potassium nutrition and rice drought tolerance. *Journal of Experimental Botany*, **67**, 2689–2698.

Ahn, S.J., Shin, R., Schachtman, D.P. (2004) Expression of KT/KUP genes in *Arabidopsis* and the role of root hairs in K+ uptake. *Plant Physiology,* **134**, 1135–1145.

Altschul, S.F., Wootton, J.C., Gertz, E.M., Agarwala, R., Morgulis, A., Schaffer, A.A., et al. (2005) Protein database searches using compositionally adjusted substitution matrices. *FEBS Journal,* **272**, 5101.

An, S., Park, S., Jeong, D-H., Lee, D-Y., Kang, H-G., Yu, J-H., Hur, J., Kim, S-R., Kim, Y-H., Lee, M., et al. (2003) Generation and analysis of end sequence database for T-DNA tagging lines in rice. *Plant Physiology,* **133**, 2040–2047.

Anderson, J.A., Huprikar, S.S., Kochian, L.V., Lucas, W.J., Gaber, R.F. (1992) Functional expression of

a probable *Arabidopsis thaliana* potassium channel in *Saccharomyces cerevisiae. Proceedings of the National Academy of Sciences USA*, **89**, 3736–3740.

Armengaud, P., Breitling, R., Amtmann, A. (2004) The potassiumdependent transcriptome of Arabidopsis reveals a prominent role of jasmonic acid in nutrient signaling. *Plant Physiology,* **136**, 2556–2576.

Bei, Q.X., Luan, S. (1998) Functional expression and characterization of a plant K channel gene in a plant cell model. *Plant Journal*, **13**, 857–865.

Bensmihen, S. (2015) Hormonal control of lateral root and nodule development in legumes. *Plants*, **4**(3), 523-547.

Cao, M.J., Yu, H.Q., Yan, H.K. (2007) Difference in Tolerance to Potassium Deficiency between Two Maize Inbred Lines. *Plant Production Science*, **10**, 42-46.

'Cao, Y., Ward, J.M., Kelly, W.B., Ichida, A.M., Gaber, R.F. et al. (1995) Multiple genes, tissue specificity, and expression-dependent modulation contribute to the functional diversity of potassium channels in *Arabidopsis thaliana. Plant Physiology,* **109**, 1093–1106.

Cherel, I., Lefoulon, C., Boeglin, S.H. (2014) Molecular mechanisms involved in plant adaptation to low Kþ availability. *Journal of Experimental Botany*, **65**, 833–848.

Chrispeels, M.J., Crawford, N.M., Schroeder, J.I. (1999) Proteins for transport of water and mineral nutrients across the membranes of plant cells. *The Plant Cell*, **11**(4), 661-675.

Clarkson, D.T., Hanson, J.B. (1980) The mineral nutrition of higher plants. *Annual Review of Plant Physiology and Plant Molecular Biology*, **31**, 239–298.

Cowperthwaite, M., Park, W., Xu, Z., Yan, X., Maurais, S.C., Dooner, H.K. (2002) Use of the transposon Ac as a gene-searching engine in the maize genome. *Plant Cell*, **14**, 713–726.

Dennison, K.L., Robertson, W.R., Lewis, B.D., Hirsch, R.E., Michael, R.S., Spalding, E.P. (2001) Functions of AKT1 and AKT2 potassium channels determined by studies of single and double mutants

of arabidopsis. *Plant Physiology*, **127**, 1012-1019.

D'Erfuth, I., Cosson, V., Eschtruth, A., Lucas, H., Kondorosi, A., Ratet, P. (2003) Efficient transposition of the *Tnt*1 tobacco retrotransposon in the model legume *Medicago truncatula. Plant Journal*, **34**, 95–106.

Dreyer, I., Michard, E., Lacombe, B., Thibaud, J.B. (2001) A plant Shaker-like K+ channel switches between two distinct gating modes resulting in either inward-rectifying or 'leak' current. *FEBS Letters*, **505**, 233–239.

Ehrhardt, D.W., Atkinson, E.M., Long, S.R. (1992) Depolarization of alfalfa root hair membrane potential by Rhizobium meliloti Nod Factors. *Science*, **256**(5059), 998–1000.

El-sherif, N., Ibrahim, M. (2020) Implications of rbcL and rpoC1 DNA barcoding in phylogenetic relationships of some Egyptian *Medicago sativa* L. cultivars. *Egyptian Journal of Botany*, **60**, 451-460.

Galibert, F., Finan, T.M., Long, S.R., Pühler, A., Abola, P., Ampe, F., et al. (2001) The composite genome of the legume symbiont *Sinorhizobium meliloti. Science*, **293**, 668–672.

Gruber, B.D., Giehl, R.F., Friedel, S., Wiren, N.V. (2013) Plasticity of the Arabidopsis root system under nutrient deficiencies. *Plant Physiology,* **163**, 161–179.

Herbert, H.H., Walter, A.A. (1972) Selective detection of organometallics in gas chromatographic effluents by flame photometry. *Journal of Chromatography A,* **74**(2),311-318.

Hirsch, D., Stahl, A., Lodish, H.F. (1998) A family of fatty acid transporters conserved from mycobacterium to man. *Proceedings of the National Academy of SciencesUSA*, **95**(15), 8625-9.

Hodge, A. (2004) The plastic plant: Root responses to heterogeneous supplies of nutrients. *New Phytologist*, **162**, 9–24.

Jan, L.Y., Jan, Y.N. (1992) Tracing the roots of ion channels. *Cell*, **69**, 715-718.

Jin, J.Y. (2012) Changes in the Efficiency of Fertiliser Use in China. *Journal of the Science of Food and Agriculture*, **92**, 1006-1009.

Kellermeier, F., Chardon, F., Amtmann, A. (2013) Natural variation of Arabidopsis root architecture reveals complementing adaptive strategies to potassium starvation. *Plant Physiology,* **161**, 1421–1432.

Lacombe, B., Pilot, G., Michard, E., Gaymard, F., Sentenac, H., Thibaud, J.-B. (2000) A shaker-like K+ channel with weak rectification is expressed in both source and sink phloem tissues of Arabidopsis. *Plant Cell*, **12**, 837–851.

Lagarde, D., Basset, M., Lepetit, M., Gaymard, F., Astruc, S., Grignon, C. (1996) Tissue-specific expression of Arabidopsis AKT1 gene is consistent with a role in K nutrition. *Plant Journal*, **9**, 195–203.

Loutfy, N., Azooz, M., Hassanein, Ahmed M., Bassiony, A. (2019) Potassium synergize the positive effect of ascorbic acid on some morpho-physiological parameters of salt stressed faba bean cultivars. *Egyptian Journal of Botany*, **59**, 735-751.

Marschner, H., Marschner, P. (2011) "*Marschner's Mineral Nutrition of Higher Plants*". Academic Press. , London, UK.

Mathieu, M., Winters, E.K., Kong, F., Wan, J., Wang, S., Eckert, H., Luth, D., Paz, M., Donovan, C., Zhang, Z., et al (2009) Establishment of a soybean (*Glycine max* Merr. L) transposon-based mutagenesis repository. *Planta*, **229**, 279–289.

Pettigrew, W.T. (2008) Potassium influences on yield and quality production for maize, wheat, soybean and cotton. *Physiologia Plantarum*, **133**, 670-681.

Pislariu, C.I., Murray, J.D., Wen, J., Cosson, V., Muni, R.R., et al. (2012) A *Medicago truncatula* tobacco retrotransposon insertion mutant collection with defects in nodule development and symbiotic nitrogen fixation. *Plant Physiology,* **159**, 1686–1699.

Prayitno, J., Rolfe, B.G., Mathesius, U. (2006) The ethylene-insensitive sickle mutant of *Medicago truncatula* shows altered auxin transport regulation during nodulation. *Plant Physiology,* **142**, 168–180.

Qi, Z., Hampton, C.R., Shin, R., Barkla, B.J., White, P.J., Schachtman, D.P. (2008) The high affinity K+ transporter AtHAK5 plays a physiological role in planta at very low K+ concentrations and provides a caesium uptake pathway in *Arabidopsis*. *Journal of Experimental Botany*, **59**, 595–607.

Ratet, P., Porcedu, A., Tadege, M., Mysore, K.S. (2006) Insertional mutagenesis in Medicago truncatula using Tnt1 retrotransposon. In U Mathesius, EP Journet, LW Sumner, eds, The Medicago truncatula handbook. http://www.noble.org/ MedicagoHandbook/ (December 3, 2012)

Ru' zicka, K., Ljung, K., Vanneste, S., Podhorska´, R., Beeckman, T., Friml, J., Benkova´, E. (2007) Ethylene regulates root growth through effects on auxin biosynthesis and transport-dependent auxin distribution. *The Plant Cell*, **19**, 2197–2212.

Schnabel, E., Journet, E. Pascal, de Carvalho-Niebel, Fernanda, Dug, G., Frugoli, J. (2005) The *Medicago truncatula* SUNN gene encodes a CLV1-like leucine-rich repeat receptor kinase that regulates nodule number and root length. *Plant Molecular Biology*, **58**(6), 809–822.

Schroeder, J.I., Ward, J.M., Gassmann, W (1994) Perspectives on the physiology and structure of inward-rectifying Kþ channels in higher plants: Biophysical implications for Kþ uptake. *Annual Review of Biophysics and Biomolecular Structure,* **23**, 441–47.

Sentenac, H., Bonneaud, N., Minet, M., Lacroute, F., Salmon, J.M., Gaymard, F., Grognon, C. (1992) Cloning and expression in yeast of a plant potassium ion transport system. *Science,* **256**, 663–665.

Shin, R., Schachtman, D.P. (2004) Hydrogen peroxide mediates plant root cell response to nutrient deprivation. *Proceedings of the National Academy of Sciences,* **101**, 8827–8832.

Spalding, E.P., Hirsch, R.E., Lewis, D.R., Qi, Z., Sussman, M.R., Lewis, B.D. (1999) Potassium uptake supporting plant growth in the absense of AKT1 channel activity: inhibition by ammonium and stimulation by sodium. *Journal of General Physiology*, **113**, 909–918.

Stepanova, A.N., Hoyt, J.M., Hamilton, A.A., Alonso, J.M. (2005) A link between ethylene and auxin uncovered by the characterization of two root specific ethylene-insensitive mutants in Arabidopsis. *Plant Cell*, **17**, 2230–2242.

Sun, L., Gill, U.S., Nandety, R.S., Kwon, S., Mehta, P.,

Dickstein, R., et al. (2019) Genome-wide analysis of flanking sequences reveals that *Tnt*1 insertion is positively correlated with gene methylation in *Medicago truncatula. The Plant Journal*, **2019**, doi: 10.1111/tpj.14291.

Szyroki, A., Ivashikina, N., Dietrich, P., Roelfsema, M. R., Ache, P. et al. (2001) KAT1 is not essential for stomatal opening. *Proceedings of the National Academy of Sciences USA*, **98**, 2917–2921.

Tadege, M., Wen, J., He, J., Tu, H., Kwak, Y., Eschstruth, A., et al. (2008) Large-scale insertional mutagenesis using the *Tnt*1 retrotransposon in the model legume *Medicago truncatula. Plant Journal,* **54**, 335–47.

Wang, X.P., Chen, L.M., Liu, W.X., Shen, L.K., Wang, F.L., Zhou, Y., Zhang, Z.D., Wu, W.H., Wang, Y. (2016) AtKC1 and CIPK23 synergistically modulate AKT1-mediated low-potassium stress responses in Arabidopsis. *Plant Physiology,* **170**, 2264–2277.

Wang, Y., Wu, W.H. (2013) Potassium transport and signaling in higher plants. *Annual Review of Plant Biology*, **64**, 451–476.

Xu, J., Li, H.D., Chen, L.Q., Wang, Y., Liu, L.L., He, L., Wu, W.H. (2006) A protein kinase, interacting with two calcineurin B-like proteins, regulates Kþ transporter AKT1 in Arabidopsis. *Cell*, **125**, 1347–1360.

Zygophyllaceae, T., Elkamali, H.H., Eltahir, A.S., Yousif, I.S., Mohamed, A., Khalid, H., Elneel, E.A. (2016) Comparative anatomical study of the stems and leaflets of *Tribulus longipetalous, T. pentandrus* and *T. terrestris* (Zygophyllaceae). *Plant Science,* **3**, 1-6.

طفرة جديدة لنبات *Medicago truncatula* تحتوى على نسخة مطفرة من جين ال AKT1 تؤدى خلل فى امتصاص البوتاسيوم والصوديوم و ظهور عقيدات جذرية مطفرة

ناهد عبد الغفار عبد العزيز ابراهيم(1)، أسماء حسن حمدى(2)، أميمة عبد العاطى شرف(3)، محمد عيد سعد(2، 4)، شيرين فؤاد الخولى(5، 6)، غادة أحمد أبو الهيبة(2)

(1) قسم الميكروبيولوجيا الجزيئية ـ معهد بحوث الهندسة الوراثية الزراعية- مركز البحوث الزراعية-جيزة- مصر، (2)قسم كيمياء الاحماض النوويه و البروتين- معهد بحوث الهندسة الوراثية الزراعية- مركز البحوث الزراعية -جيزة- مصر، (3)قسم الميكروبيولوجيا ـ المركز القومي للبحوث الطبية ـ الدقي ـ الجيزة ـ مصر، (4)قسم الأحياء ـ كلية العلوم ـ جامعة طيبة ـ المدينة المنورة ـ المملكة العربية السعودية، (5)قسم الأحياء ـ كلية العلوم والدراسات الأنسانية ـ جامعة الأمير سطام بن عبد العزيز ـ 11942 الخرج ـ المملكة العربية السعودية، (6)قسم البيولوجيا الجزيئية للنبات- معهد بحوث الهندسة الوراثية الزراعية- مركز البحوث الزراعية ـجيزة- مصر.

تم استخدام النهج الجيني العكسي لعزل وتوصيف صنف من نبات الفصة البرميلية *Medicago truncatula* التي تحتوي على طفرة فى جين من الجينات المسئولة عن تكوين العقد الجذرية وأدى ذلك إلى تغييرات فـسيولوجية. تم عزل أكثر من 60 علامة تسلسل (FSTs) Tnt1-Flanking ويتراوح حجمها من 70- 600 قاعدة نيتروجينية، وتم تسلسلها و إيداعها لقاعده البيانات الجينية المطفر. تم تعيين إدخال Tnt1 المناسب في الكروموسوم رقم 8 من جينوم.*Medicago truncatula*. تم تحديده بدقة قبل القاعدة 141 وبعد شفرة البداية ATG لجين AKT1 لقناة البوتاسيوم (MtAKT1) *Medicago truncatula*. تم عزل الجين MtAKT1 المعدل داخليًا لقناة البوتاسيوم وتسلسله وإيداعه بال Genebank برقم الانضمام MN649185.1. حقق النوع المطفر *M. truncatula* akt1 mutant عددًا أكبر من العقيدات الجذرية المشوهة وطول جذر أقصر مقارنة بالصنف الطبيعي. أظهرت عقيدات akt1 حجمًا منخفضًا مشغولة بخلايا غير متمايزة وتشوهات في مناطق العقيدات التكافلية. كما لوحظت منطقة تثبيت النيتروجين غير الوظيفية ومنطقة الإصابة المضغوطة. يُظهر متحور AKT1 توهينًا في قدرته على الحفاظ على محتوى أيون K $^+$ و Na $^+$ المناسب في شتلات akt1 التي تقل بمقدار 3-2 أضعاف عن الشتلات الطبيعية. في المقابل ،أظهرت شتلات akt1 زيادة بمقدار ثلاثة أضعاف في تركيز أيونات الكالسيوم مقارنة بالصنف الطبيعي. أن هذا النبات المطفر تم بطريقة أثرت على الجينات الخاصة بقناة البوتاسيوم مما أدى إلى إختلاف استغلال الايونات وعلى عضو تثبيت النيتروجين.